InP-Based 1.3 – 1.6 μm VCSELs with Selectively Etched Tunnel-Junction Apertures on a Wavelength Flexible Platform

D. Feezell, D.A. Buell, and L.A. Coldren, *Fellow, IEEE.*

Abstract— In this paper, the authors demonstrate a wavelength flexible platform for the production of long-wavelength vertical-cavity surface-emitting lasers which provide full wavelength coverage from 1.3 – 1.6 μm. All-epitaxial InP-based devices with AsSb-based distributed Bragg reflectors were achieved through a common design, process, and growth technology at both the important telecommunications wavelengths of 1.3 μm and 1.5 μm. Thin selectively etched tunnel junctions were implemented as low-loss apertures and offer scalability to small device dimensions. Devices showed low threshold currents (< 2 mA), near single-mode (SMSR >20dB) operation, and high differential efficiency (>40% at 1.3 μm and >25% at 1.5 μm).

***Index Terms*— Vertical-cavity surface-emitting lasers, semiconductor laser processing, InP-based, optical fiber communications, tunnel junction, long wavelength, semiconductor lasers, molecular beam epitaxy.**

I. Introduction

Long wavelength vertical-cavity surface-emitting lasers (VCSELs) operating in the 1.3 – 1.6 μm wavelength range are attractive light sources for metro, local area, and storage area networks. These devices offer a potential low-cost alternative to existing distributed feedback (DFB) laser transmitters. In addition, due to simple packaging, high fiber-coupling efficiency, and on-wafer testing, VCSELs offer many inherent advantages over the existing in-plane infrastructure.

Recently, much attention has been devoted to a variety of approaches to long-wavelength VCSEL devices. Structures employing epitaxial, dielectric, and wafer bonded distributed Bragg reflector (DBR) mirrors have all been demonstrated. Various active region designs have also been utilized with success. Several of the most promising material systems include GaInNAs [1], AlInGaAs [2,3,4,5], and InGaAsP [6]. The underlying drawback to the majority of these approaches, however, is their inability to produce monolithic all-epitaxial devices that span the entire 1.3 – 1.6 μm wavelength range. From a manufacturability standpoint, this is an important goal.

Manuscript received May 5, 2005. This work was supported in part by the National Science Foundation.

The authors are with the Department of Electrical and Computer Engineering and the Department of Materials Science, University of California Santa Barbara, Santa Barbara, CA 93106 USA. (telephone: 805-893-5955, email: feezell@engineering.ucsb.edu).

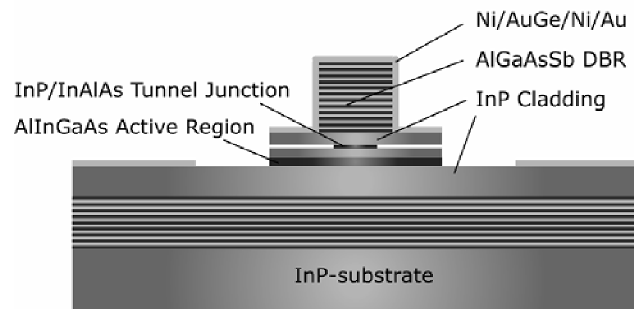

Fig. 1. Schematic of bottom-emitting all-epitaxial VCSEL structure with undercut tunnel-junction aperture.

Previously, we have reported monolithic all-epitaxial InP-based VCSELs with AlGaAsSb DBRs and AlInGaAs active regions [7,8]. AsSb-based DBRs are lattice matched to InP and offer high reflectivity over a broad wavelength range, thus enabling wavelength selection from 1.3 – 1.6 μm. In fact, the available index contrast is $\Delta n \approx 0.4$, comparable to that of the GaAs/AlGaAs system. Coupled with the mature AlInGaAs active regions, AsSb-based technology facilitates all-epitaxial InP-based devices spanning the entire long-wavelength range with consistent device design, process flow, and materials growth.

In addition, we have previously investigated several aperturing techniques [7,8,9], unfortunately these aperturing schemes have suffered from high scattering loss, difficult processing steps, or current crowding. Recently, we have demonstrated an improved aperture through selective etching of a thin tunnel junction layer to achieve simultaneous optical and electrical confinement in in-plane lasers [10].

In this letter, we report the fabrication of InP-based 1.3 μm and 1.5 μm VCSELs with AsSb-based DBRs and selectively etched tunnel-junction apertures. We demonstrate a platform with flexible lasing wavelength and low-loss apertures scalable to small dimensions. This is the first reported 1.3 μm InP-based all-epitaxial VCSEL with AsSb-based DBRs and a selectively etched tunnel-junction aperture. Finally, we show the effectiveness of the thin tunnel-junction apertures in

facilitating single mode operation, improving differential efficiency, and reducing threshold current.

II. VCSEL Design and Fabrication

Figure 1 shows a schematic of the bottom-emitting device structure applicable to both 1.3 μm and 1.5 μm devices. The VCSEL was grown by solid-source molecular beam epitaxy (MBE) in a single growth step. A double intra-cavity contacting scheme is employed to circumvent the high electrical and thermal resistances of the AsSb-Based DBRs. The ½-λ AlInGaAs active region contains five 1.0% compressively strained 7 nm quantum wells and six 0.6% tensile-strained 5 nm barriers. Cladding both sides of the active region are InP layers doped 5e17 cm^{-3} that facilitate current spreading and heat removal in the device. The upper InP cladding layer contains a 3e19 cm^{-3} n^{++}-InAlAs/ 1e20 cm^{-3} p^{++}-InP tunnel-junction layer placed at a standing wave null to minimize absorption loss, which is selectively etched to form the thin aperture. The total cavity thickness is 3.5-λ. The DBRs are $Al_{.30}Ga_{.70}As_{.53}Sb_{.47}/Al_{.95}Ga_{.05}As_{.51}Sb_{.49}$ for the 1.3μm structure and $Al_{.15}Ga_{.85}As_{.54}Sb_{.46}/Al_{.95}Ga_{.05}As_{.51}Sb_{.49}$ for the 1.5μm structure. The top and bottom mirrors contain 36.5 and 24.5 pairs for the 1.3 μm devices, respectively, and 34.5 and 24.5 pairs for the 1.5 μm devices, respectively. The major advantage of this structure is that both 1.3 μm and 1.5 μm devices are realized with parallel design, process, and materials growth technology. This is potentially an excellent platform for coarse wavelength division multiplexing (CWDM) applications between 1.3 – 1.6 μm with 20 nm channel spacing.

Device fabrication involved reactive ion etching (RIE) of the top DBR down to the top InP contact layer in Cl_2 plasma. The upper InP cladding layer, which functions as an etch-stop layer for the upper DBR, was etched down to the tunnel-junction layer via RIE with CH_4-H_2-Ar. Selective lateral etching of the InAlAs portion of the tunnel junction was then performed with a mixture of citric acid and hydrogen peroxide to form the thin air-gap aperture. The selectivity of this etch over InP was observed to be greater than 100 to 1. Subsequently, the remaining InP cladding was etched to the active region via RIE. Finally, the active region was etched with a citric acid and hydrogen peroxide mixture to expose the bottom InP contact layer. Ni/AuGe/Ni/Au was then evaporated on the top and bottom InP contact layers.

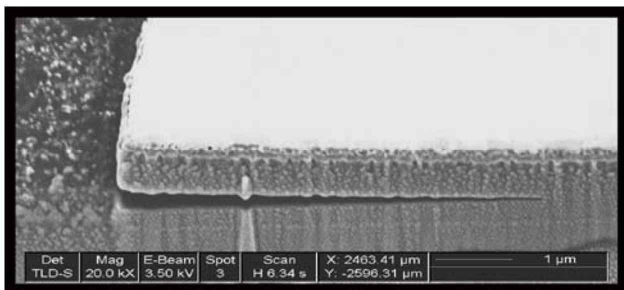

Fig. 2. Cross-sectional SEM of selectively etched InAlAs/InP tunnel-junction aperture in a VCSEL cavity test structure.

A scanning electron microscope (SEM) picture of the selectively etched tunnel-junction air-gap aperture is shown in Figure 2. The dimensions of the aperture are controlled through observing the removal of sacrificial etch pillars on the wafer.

III. Results and Discussion

1.3 μm and 1.5 μm devices were fabricated and tested. Light output versus current and voltage (LIV) curves are shown for both 1.3 μm and 1.5 μm VCSELs in Figures 3 and 4, respectively. These devices were each 20 μm diameter pillars with 8 μm diameter tunnel-junction apertures. The spectra at 3X threshold for both wavelengths are inset in the appropriate figures and demonstrate the near single-mode (SMSR >20dB) nature of these devices. This operation

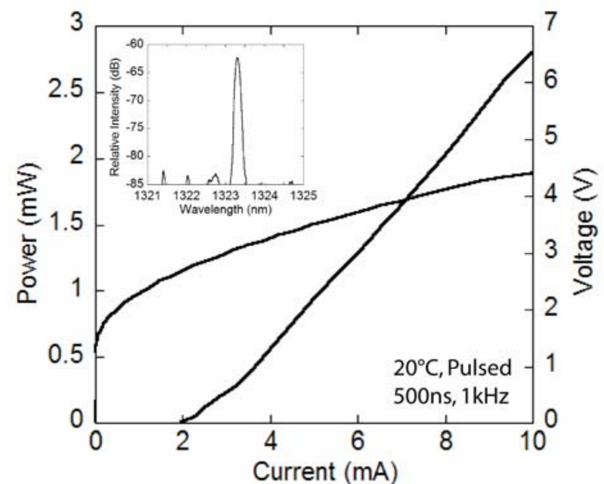

Fig. 3. Room temperature pulsed LIV curve for 1.3 μm VCSEL with inset pulsed lasing spectrum. Data was under-sampled due to pulsed measurement restrictions, giving apparent kink in LIV curve.

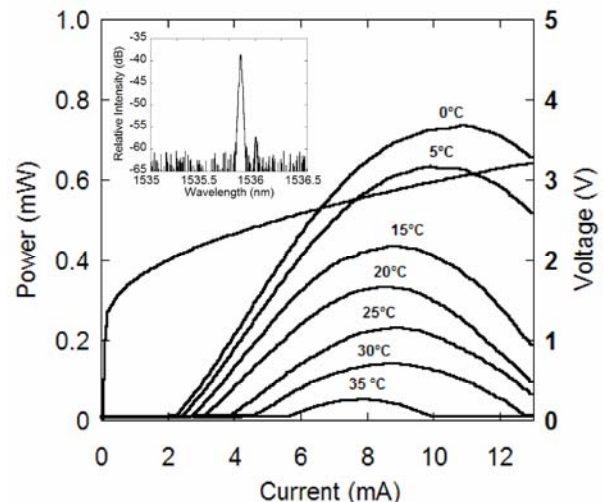

Fig. 4. Continuous wave LIV curves at various temperatures for 1.5 μm VCSEL with inset CW lasing spectrum.

demonstrates that the thin air-gap aperture placed at a standing wave null provides sufficient index contrast to confine the mode to smaller dimensions without significant scattering loss.

We believe this to be the first report of an InP-based 1.3 µm VCSEL with AsSb-based DBRs and tunnel junction aperturing technology. The 1.3 µm devices lased pulsed (20°C, 500ns, 1kHz) at 1.32 µm and showed a high differential efficiency of greater than 40%, demonstrating that

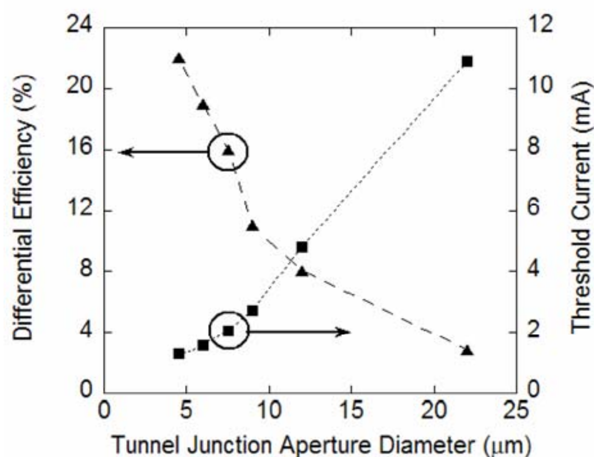

Fig. 5. Differential efficiency and threshold current vs. tunnel-junction aperture diameter for a 1.5 µm device, showing scalability of aperturing technology.

the thin tunnel-junction aperture effectively confines the optical mode away from the rough DBR sidewalls. The 1.3 µm devices only displayed continuous wave (CW) lasing at 0°C due to a red shift of the gain peak with respect to the cavity-mode and the low bottom mirror reflectivity (R ≈ 99.1%). The 1.5 µm devices lased at 1.54 µm and achieved differential efficiencies above 25%. CW operation was observed for these devices up to 35°C. Higher temperature performance is expected at both wavelengths with proper adjustment of the gain peak to cavity-mode offset.

The scalability of the thin tunnel-junction apertures to small dimensions is important for low threshold operation and to therefore reduced heat generation in the devices. Figure 5 displays an example of this scalability. A reduction in threshold current is demonstrated in a 1.5 µm device as the tunnel-junction aperture is scaled to smaller dimensions. In fact, both wavelengths of devices displayed very low threshold currents, with a lowest value of 0.67 mA for a 4 µm tunnel junction diameter in a 1.5 µm device, and a lowest value of 1.4mA for a 6 µm tunnel junction diameter in a 1.3 µm device. This result clearly indicates the effective current confinement achieved by the tunnel-junction apertures.

Figure 5 also shows a greater than 5X improvement in differential efficiency as the aperture is scaled to smaller dimensions, indicating that the thin tunnel-junction aperture achieves mode guiding down to small dimensions without introducing significant scattering loss to the device. The low differential efficiencies for large aperture sizes are due to scattering off the rough pillar sidewalls, as the aperture diameter is still comparable to the pillar diameter. These results are in good correlation with simulations based on an algorithm analogous to the classic work of Fox and Li [11].

IV. Conclusions

We have demonstrated all-epitaxial 1.3µm and 1.5µm InP-based VCSELs on a wavelength flexible platform that utilizes a common design, process, and materials growth technology. This shows excellent promise for CWDM applications. Implementation of a thin selectively etched tunnel-junction aperture provided simultaneous electrical and optical confinement and has led to near single-mode operation. These apertures have exhibited good performance down to small dimensions, generating low threshold currents and high differential efficiencies. Future work will involve optimization of the gain peak to cavity-mode offset and high-speed characterization.

References

[1] T. Nishida, M. Takaya, S. Kakinuma, T. Kaneko, and T. Shimoda, “4.2mW GaInNAs long-wavelength VCSEL grown by metalorganic chemical vapor deposition,” *IEEE Semiconductor Laser Conference,* Matsue-shi, Japan, Sept 2004.

[2] V. Jayaraman. M. Mehta, A.W. Jackson, S. Wu, Y. Okuno, J. Piprek, and J.E. Bowers, “High-Power 1320-nm Wafer-Bonded VCSELs With Tunnel Junctions,” *IEEE Photon. Technol. Lett.,* vol. 15, no. 11, pp.1495-1497, Nov.2004.

[3] N. Nishiyama, C. Caneau, B. Hall, G. Guryanov, M. Hu, X. Liu, R. Bhat, and C. Zah, “Temperature, Modulation, and Reliability Characteristics of 1.3µm-VCSELs on InP with AlGaInAs/InP Lattice Matched DBR,” *IEEE Semiconductor Laser Conference,* Matsue-shi, Japan, Sept 2004.

[4] J. Chang, C.L. Shieh, X. Huang, G. Liu, M.V.R. Murty, C.C. Lin, and D.X. Xu, “Efficient CW Lasing and High-Speed Modulation of 1.3−µm AlGaInAs VCSELs With Good High Temperature Lasing Performance,” *IEEE Photon. Technol. Lett.,* vol. 17, no. 1, pp. 7-9, Jan 2005.

[5] R. Shau, M. Ortsiefer, J. Rosskopf, G. Bohm, F. Kohler, and M.C. Amann, “Vertical-cavity surface-emitting laser diodes at 1.55µm with large output power and high operation temperature,” *Elect. Lett.,* vol. 37, no. 21, pp. 1295-1296, Oct 2001.

[6] C.K. Lin, D.P. Bour, J. Zhu, W.H. Perez, M.H. Leary, A. Tandon, S.W. Corzine, and M.R.T. Tan, “Long wavelength VCSELs with InP/air-gap DBRs,” *SPIE Int. Soc. Opt. Eng. Proceedings,* vol. 5364, no. 1, pp. 16-24, 2004.

[7] S. Nakagawa, E. Hall, G. Almuneau, J.K. Kim, D.A. Buell, H. Kroemer, and L.A. Coldren, “88°C, continuous-wave operation of apertured, intracavity contacted, 1.55µm vertical-cavity surface-emitting lasers,” *Appl. Phys. Lett.,* vol. 78, pp. 1337-1339, 2001.

[8] T. Asano, D. Feezell, R. Koda, M.H.M. Reddy, D.A. Buell, A.S. Huntington, E. Hall, S. Nakagawa, and L.A. Coldren, “InP-Based All-Epitaxial 1.3µm VCSELs With Selectively Etched AlInAs Apertures and Sb-Based DBRs,” *IEEE Photon. Technol. Lett.,* vol. 15, no.10, pp.1333-1335, Oct 2003.

[9] M.H.M. Reddy, D.A. Buell, T. Asano, R. Koda, D. Feezell, A.S. Huntington, and L.A. Coldren, “Lattice-matched $Al_{0.95}Ga_{0.05}AsSb$ oxide for current confinement in InP-based long wavelength VCSELs,” *Journal of Crystal Growth*, vol.251, no.1-4, pp. 766-770, Apr 2003.

[10] M.H.M. Reddy, T. Asano, D. Feezell, D.A. Buell, A.S. Huntington, R. Koda, and L.A. Coldren, “Selectively Etched Tunnel Junction for Lateral Current and Optical Confinement in InP-Based Vertical Cavity Lasers,” *Jour. of Elec. Mat.,* vol. 33, no. 2, pp. 118-122, 2004.

[11] A.G. Fox and T. Li, "Resonant Modes in a Maser Interferometer," *Bell Syst. Tech. Journal,* vol. 40, pp. 453-488, 1961.